J|A|C|S
ARTICLES
Published on Web 05/23/2002

Selective Formation of Cumulative Double Bonds (C═C═N) in the Attachment of Multifunctional Molecules on Si(111)-7 × 7

Feng Tao, Xian Feng Chen, Zhong Hai Wang, and Guo Qin Xu*

Contribution from the Department of Chemistry, National University of Singapore, 10 Kent Ridge, Singapore, 119260

Received November 19, 2001

Abstract: The cumulative double bond (C═C═N), an important intermediate in synthetic organic chemistry, was successfully prepared via the selective attachment of acrylonitrile to Si(111)-7 × 7. The covalent binding of acrylonitrile on Si(111)-7 × 7 was studied using high-resolution electron energy loss spectroscopy (HREELS), X-ray photoelectron spectroscopy (XPS), ultraviolet photoelectron spectroscopy (UPS), scanning tunneling microscopy (STM) and DFT calculations. The observation of the characteristic vibrational modes and electronic structures of the C═C═N group in the surface species demonstrates the [4 + 2]-like cycloaddition occurring between the terminal C and N atoms of acrylonitrile and the neighboring adatom−rest atom pair, consistent with the prediction of DFT calculations. STM studies further show the preferential binding of acrylonitrile on the center adatom sites of faulted halves of Si(111)-7 × 7 unit cells.

I. Introduction

The marriage of organic functionalities with silicon-based device technologies has recently attracted much attention, possibly enabling us to design and create hybrid silicon−molecular electronics. It offers potential opportunities to combine high chemical, mechanical, and thermal stabilities with tailored electronic or optical properties into existing device technologies.[1−5] In addition, the reactions of organic molecules with silicon surfaces play important roles in preparing silicon−organic thin films.[6−8] For example, covalently bound organic monolayers may be employed as an intermediate for further reacting with different/same organic molecules to form ultrathin organic films, particularly feasible if the monolayers possess a variety of chemical functionalities. To establish the molecular linkages at the interfaces, it is important to understand the reactivity and selectivity of organic functionalities with silicon surfaces.

One of the most important and well-understood semiconductor surfaces is Si(111)-7 × 7. Its structure can be described by the dimer-adatom-stacking (DAS) fault model proposed by Takayanagi et al.,[9] shown in Figure 1. This surface provides a number of chemically, spatially, and electronically inequivalent reactive sites, including the adatoms and rest atoms in the inherently different faulted and unfaulted halves and corner holes. Previous studies[10−15] show that the adjacent adatom−rest atom pair can serve as a reactive functional group to readily react with unsaturated organic functionalities.

On the other hand, in organic syntheses, vinyl and cyano groups are two of the most important building blocks for many organic molecules.[16] Acrylonitrile, a typical monomer with both vinyl and cyano groups, is a valuable polyfunctional heteroatomic molecule having single, double, and triple bonds. The cyano group modifies the electronic structure of the vinyl group through conjugation. Regarded as a substituted ethylene due to conjugative and inductive effects, acrylonitrile possesses both electron-withdrawing and electron-donating properties,[17] indicative of its rich chemistry. Thus, as a typical multifunctional molecule, exploring its selective binding on Si(111)-7 × 7 will provide the correlation of reactivity and selectivity of multifunctional molecules with electronic and geometric structures of Si surface dangling bonds and will offer the necessary flexibility in the functionalization and modification of silicon surfaces.

* To whom correspondence should be addressed. Fax: (65) 779-1691. E-mail: chmxugq@nus.edu.sg.

(1) Yates, J. T., Jr. *Science* **1998**, *279*, 335−336.
(2) Hamers, R. J.; Coulter, S. K.; Ellison, M. D.; Hovis, J. S.; Padowitz, D. F.; Schwartz, M. P.; Greenlief, C. M.; Russell, J. N. *Acc. Chem. Res.* **2000**, *33*, 617−624.
(3) Wolkow, R. A. *Annu. Rev. Phys. Chem.* **1999**, *50*, 413−441.
(4) Waltenburg, H. N.; Yates, J. T., Jr. *Chem. Rev.* **1995**, *95*, 1589−1673
(5) Hamers, R. J.; Wang, Y. *Chem. Rev.* **1996**, *96*, 1261−1290.
(6) He, J.; Patitsas, S. N.; Preston, K. F.; Wolkow, R. A.; Wayner, D. D. M. *Chem. Phys. Lett.* **1998**, *286*, 508−514.
(7) Fuchs, H.; Ohst, H.; Prass, W. *Adv. Mater.* **1991**, *3*, 10−18.
(8) Forrest, S. R. *Chem. Rev.* **1997**, *97*, 1793−1896.
(9) Takayanagi, K.; Tanishiro, T.; Tanahashi, S.; Takahashi, M. *J. Vac. Sci. Technol. A* **1985**, *3*, 1502−1506.
(10) Rochet, F.; Jolly, F.; Bournel, F.; Dufour, G.; Sirotti, F.; Cantin, J. L. *Phys. Rev. B* **1998**, *58*, 11029−11042.
(11) Rochet, F.; Dufour, G.; Prieto, P.; Sirotti, F.; Stedile, F. C. *Phys. Rev. B* **1998**, *57*, 6738−6748.
(12) Cao, Y.; Wang, Z. H.; Deng, J. F.; Xu, G. Q. *Angew. Chem. Int. Ed.* **2000**, *39*, 2740−2742.
(13) Cao, Y.; Yong, K. S.; Wang, Z. Q.; Chin, W. S.; Lai, Y. H.; Deng, J. F.; Xu, G. Q. *J. Am. Chem. Soc.* **2000**, *122*, 1812−1813.
(14) Cao, Y.; Wei, X. M.; Chin, W. S.; Lai, Y. H.; Deng, J. F.; Bernasek, S. L.; Xu, G. Q. *J. Phys. Chem. B* **1999**, *103*, 5698−5702.
(15) Cao, Y.; Deng, J. F.; Xu, G. Q. *J. Chem. Phys.* **2000**, *112*, 4759−4767.
(16) Morrison, R. T.; Boyd, R. N. *Organic Chemistry*; Allyn and Bacon: Boston, 1959.
(17) Daimay, L. V.; Norman, B. C.; William, G. F.; Jeanette, G. G. *The Handbook of Infrared and Raman Characteristic Frequencies of Organic Molecules*; Academic Press: Boston, 1991.

10.1021/ja012563w CCC: $22.00

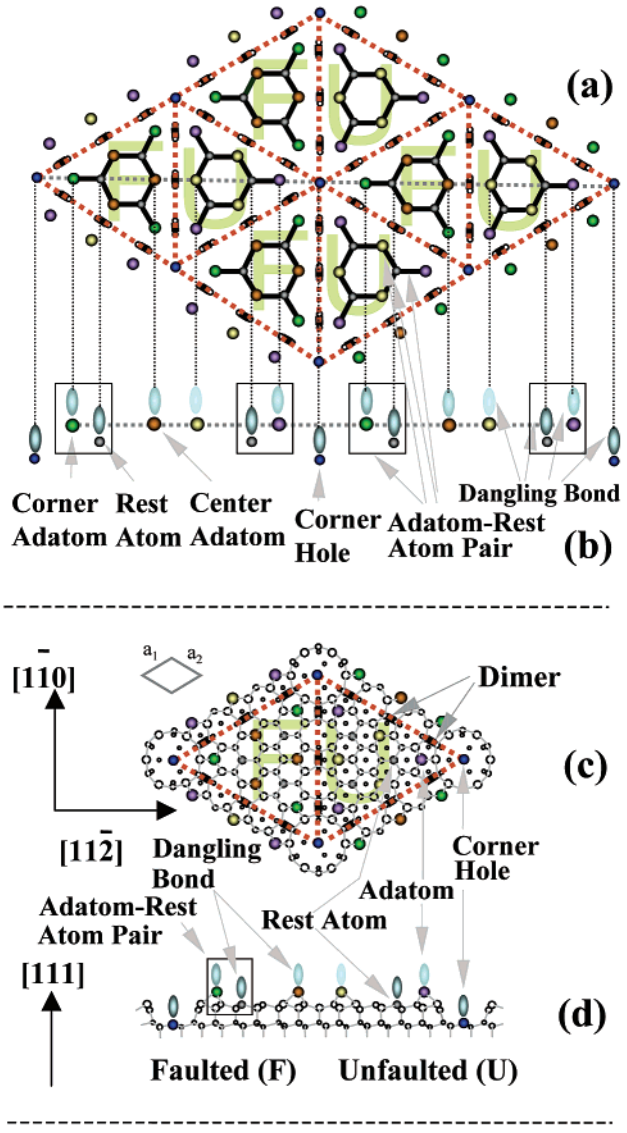

Figure 1. Top (a) and side (b) views of reactive adatoms and rest atoms of four Si(111)-7 × 7 unit cells and top (c) and side (d) views of the detailed structure on the basis of dimer-adatom-stacking (DAS) fault 7 × 7 model.

In this paper, the covalent attachment chemistry of acrylonitrile on Si(111)-7 × 7 was studied with the objectives of elucidating the acrylonitrile/Si(111)-7 × 7 interfacial reaction mechanism and developing a functional intermediate suitable for further organic syntheses and functionalization. High-resolution electron energy loss spectroscopy (HREELS) was used to characterize the vibrational properties of acrylonitrile on Si(111)-7 × 7. X-ray photoelectron spectroscopy (XPS) provides information on chemical shifts of the C 1s and N 1s core levels. The valence band structures of the adlayers were probed with ultraviolet photoelectron spectroscopy (UPS). Scanning tunneling microscopy (STM) was employed to investigate the spatial distribution and selectivity of this surface reaction system at atomic resolution. DFT calculations (*p*BP/DN** in Spartan 5.1) were commanded to optimize the chemisorption geometries and calculate their adsorption energies and vibrational frequencies. Our experimental results, together with DFT calculations, show that acrylonitrile is covalently bonded to Si(111)-7 × 7 mainly through a [4 + 2]-like cycloaddition of the C═C−C≡N skeleton with the adjacent adatom−rest atom pair. The formed cumulative double bonds C═C═N may be considered as a precursor for further organic syntheses[18] and modification of silicon surfaces.

II. Experimental Section

The experiments were performed in three separate ultrahigh vacuum (UHV) systems with a base pressure lower than 2×10^{-10} Torr. The investigation of vibrational properties was carried out in a HREELS (LK2000-14R) chamber. The HREELS spectrometer consists of a double-pass 127° cylindrical deflector analyzer (CDA) as the monochromator and a single-pass 127° CDA for the energy analysis. HREELS spectra were taken in a specular geometry on both the clean and acrylonitrile adsorbed samples with a primary beam energy of 5.0 eV. A resolution of ~40 cm^{-1} (full width at half-maximum for the elastic peak) can be routinely achieved. The C 1s and N 1s core levels and valence band structure of acrylonitrile on Si(111)-7 × 7 were obtained on another UHV system mounted with a dual-anode X-ray gun, electron energy analyzer (CLAM 2, VG) and a He UV lamp. In the XPS experiments, the Mg X-ray source ($h\nu$ = 1253.6 eV) was used. All of the spectra presented in this paper are referenced to the binding energy (BE) of 99.3 eV[19] for the bulk Si2p XPS peak. The spectra of the physisorbed multilayer and saturated chemisorption monolayer were fitted with the software VGX900 (VG Scientific, U.K.). During the fitting, the full width at half-maximum (fwhm) of each peak was kept at 1.2 eV, which is the typical resolution of the C 1s core level for our XPS system. For a wider energy window, He II photons (40.80 eV) were employed in UPS studies. The STM images were collected in the third UHV chamber equipped with a scanning tunneling microscope (Omicron) and a low-energy electron diffraction spectrometer (LEED) (Perkin-Elmer).

The Si(111) samples (9 × 18 × 0.38 mm) were cut from *n*-type (*P*-doped) silicon wafers with a resistivity of 1−30 Ω·cm and purity of 99.999% (Goodfellow). A Ta foil with a thickness of 0.025 mm was sandwiched between two identical samples with a set of Ta clips and, in turn, was spot-welded to two Ta posts (diameter ~1.5 mm) at the bottom of a Dewar-type LN_2-cooled sample holder. The sample was heated through resistive heating of the sandwiched Ta foil. It was carefully cleaned by cycles of Ar^+ sputtering and annealing to 1200 K. Acrylonitrile (99%, Aldrich) and acrylonitrile-2-d_1 (98%, C/D/N Isotopes Inc.) were further purified by several freeze−pump−thaw cycles before being dosed onto the silicon surface through a Varian adjustable leak valve. Exposures were calculated and reported in Langmuir (1 L = 10^{-6} Torr·s) without ion gauge sensitivity calibration.

III. Results

III A. High-Resolution Electron Energy Loss Spectroscopy. Figure 2 shows the high-resolution electron energy loss spectra of Si(111)-7 × 7 exposed to acrylonitrile (C^3H_2═C^2H−C^1≡N) at 110 K. The vibrational frequencies and their assignments for physisorbed and chemisorbed molecules are listed in Table 1. This table clearly shows that the vibrational features of physisorbed acrylonitrile (Figure 2b,c) are in excellent agreement with the IR spectrum of liquid acrylonitrile as well as the previous IR studies of acrylonitrile physisorbed on transition metals.[20−22] Among these vibrational signatures, the

(18) Patai, S. *The Chemistry of Ketenes, Allenes and Related Compounds*; John Wiley & Sons: Chichester−New York−Brisbane−Toronto, 1980.
(19) Moulder, J. F.; Stickle, W. F.; Sobol, P. E.; Bomben, K. D. *Handbook of X-ray Photoelectron Spectroscopy*; Physical Electronics Division, Perkin-Elmer Corporation: Minnesota, 1991.
(20) Halverson, F.; Stamm, R. F.; Whalen, J. J. *J. Chem. Phys.* **1948**, *16*, 808−816.
(21) Kubota, J.; Kondo, J.; Domen, K.; Hirose, C. *J. Electron. Spectrosc. Relat. Phenom.* **1993**, *64/65*, 137−144.
(22) Parent, P.; Laffon, C.; Tourillon, G.; Cassuto, A. *J. Phys. Chem.* **1995**, *99*, 5058−5066.

Table 1. Assignments of Physisorbed and Chemisorbed Acrylonitrile on Si(111)-7 × 7[a]

vibrational assignments	liquid-phase IR[20]	physisorbed CH_2=CH–CN on Si(111)–7 × 7	vibrational assignments	chemisorbed CH_2=CH–CN/CH_2=CDCN on Si(111)-7 × 7	calculated vibrational frequencies for CH_2=CH–CN/Si(111)-7 × 7
$=CH_2$ asymmetric stretch	3114, 3091	3102	$=CH_2$ stretch		
=CH stretch	3033	3032	−CH(D)= stretch	3034/2296	3011
$=CH_2$ symmetric stretch	2990	−	$-CH_2-$ stretch	2938/2935	2912
C≡N stretch	2228	2239	C=C=N asymmetric stretch	2032/2028	2024
C=C stretch	1609	1615	-CH_2- scissors	1398/1396	1380
CH_2 deformation	1415	1402	C=C=N symmetric stretch	1167/1158	1151
CH_2 scissors	1376		C=C=N torsion	835/868	
CH_2 wag	1325	1297	C=C=N bend	607/615	585 (off-plane), 615 (in-plane)
=CH bend	1288		Si−C/Si−N stretch	∼490/∼480	506
CH_2 twist	1215	1128			
$=CH_2$ rock	1094				
$=CH_2$ twist	960	967			
CH_2 rock	980				
C−C−C symmetric stretch	871	885			
C=C torsion	690	624			
C=C−C bend	570				

[a] All frequencies are in cm^{-1}

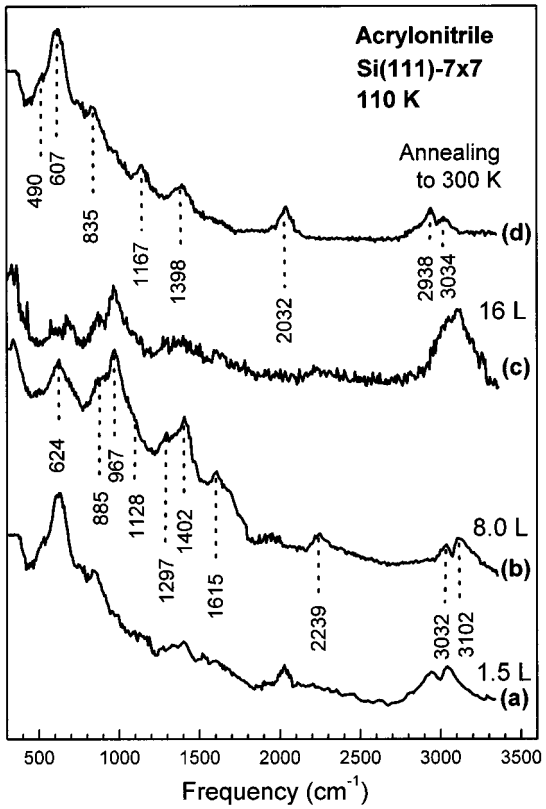

Figure 2. HREELS spectra as a function of acrylonitrile exposure at 110 K (a, b, and c) and the saturated chemisorption monolayer (d) on Si(111)-7 × 7.

two peaks at 3102 and 3032 cm^{-1} are assigned to the C−H stretching modes of the C^3H_2= and $-C^2H$= groups, respectively. The features at 1615 and 2239 cm^{-1} are related to the C^3=C^2 and C^1≡N stretching modes, respectively.

The vibrational features of chemisorbed acrylonitrile at low exposures (Figures 2a) or obtained by annealing the multilayer acrylonitrile-exposed sample to 300 K to drive away all the physisorbed molecules and retain only the chemisorbed molecules (Figure 2d), however, are significantly different. Losses at 490, 607, 835, 1167, 1398, 2032, 2938, and 3034 cm^{-1} can be readily resolved. The disappearance of the C^1≡N stretching around 2239 cm^{-1} in chemisorbed molecules strongly suggests the involvement of the C^1≡N group in the surface binding. Compared to physisorbed molecules with C−H stretching at 3102 cm^{-1} (C^3H_2=) and 3032 cm^{-1} ($-C^2H$=), the two vibrational peaks at 2938 and 3034 cm^{-1} for chemisorbed molecules are attributable for (sp^3)C−H and (sp^2)C−H stretching modes, respectively, demonstrating the rehybridization of carbon atom and the direct participation of the C^3=C^2 group in the surface reaction. Another major change is the appearance of a new peak at 2032 cm^{-1}, ascribed to the characteristic vibration of a C^2=C^1=N skeleton (asymmetic stretching mode).[23−25] This assignment was further supported by the observation of the symmetric stretching, torsion, and bend modes of C^2=C^1=N at 1167, 835, and 607 cm^{-1}, respectively.[23−25] The vibrational feature at ∼1398 cm^{-1} is attributed to $-C^3H_2-$ scissor mode, which will be further proved by the following HREELS studies of acrylonitrile-2-d_1. The broad vibrational band around 490 cm^{-1} is associated with the Si−C and Si−N stretching, consistent with the previous studies on the binding of unsaturated N-containing organic molecules on a Si surface.[23,26−27] The detailed assignments are tabulated in Table 1. The main vibrational features of chemisorbed acrylonitrile correlates well with those of ketenimine CH_2=C=NH containing the same skeleton of C=C=N.[24]

To further confirm our assignments, acrylonitrile-2-d_1 adsorption was also studied in our HREELS experiments. Figure 3 presents the vibrational features of the physisorbed acrylonitrile-2-d_1 and the saturated chemisorption molecules on Si(111)-7 × 7. Compared to the physisorbed C^3H_2=C^2H−C^1≡N (Figure 2b), the vibrational spectrum of physisorbed C^3H_2=C^2D−C^1≡N in Figure 3a presents a new peak at 2298 cm^{-1} that is assigned to C^2−D stretching of the =C^2D− group, in addition to the peaks at 3002 and 3101 cm^{-1} (C^3−H stretching modes of C^3H_2=). Upon chemisorption, the C^2−D stretching mode of $-C^2D$= remains at the same vibrational frequency, retaining sp^2 hybridization for the C^2 atom. The C^3−H stretching of C^3H_2 group, however, shifts from 3101 and 3002 cm^{-1} for physisorbed molecules to 2935 cm^{-1} for chemisorption, significant

(23) Daimay, L. V.; Norman, B. C.; William, G. F.; Feanette, G. G. *The Handbook of Infrared and Raman Characteristic Frequencies of Organic Molecules*; Academic Press: Boston, 1991.
(24) Jacox, M. E. *Chem. Phys.* **1979**, *43*, 157−167.
(25) Amatatsu, Y.; Hamada, Y.; Tsuboi, M. *J. Mol. Spectrosc.* **1987**, *123*, 476−485.

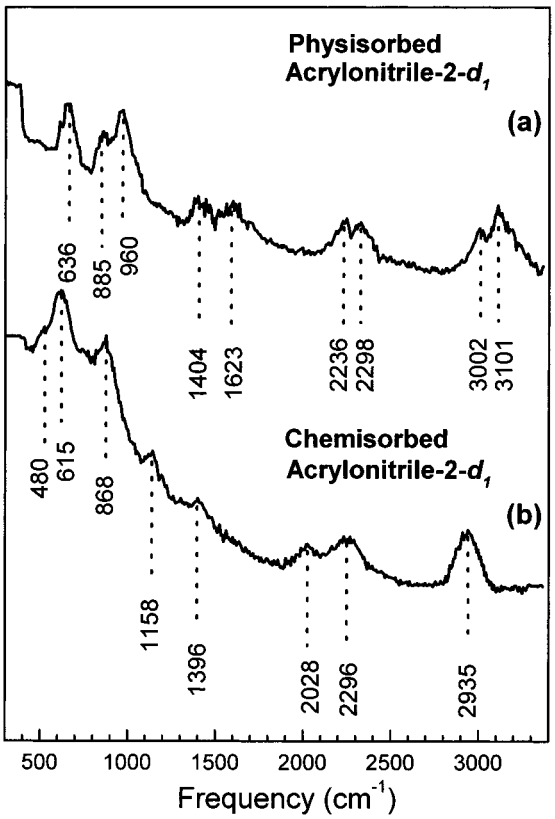

Figure 3. HREELS spectra of the physisorbed and saturated chemisorption acrylonitrile-2-d_1 on Si(111)-7 × 7.

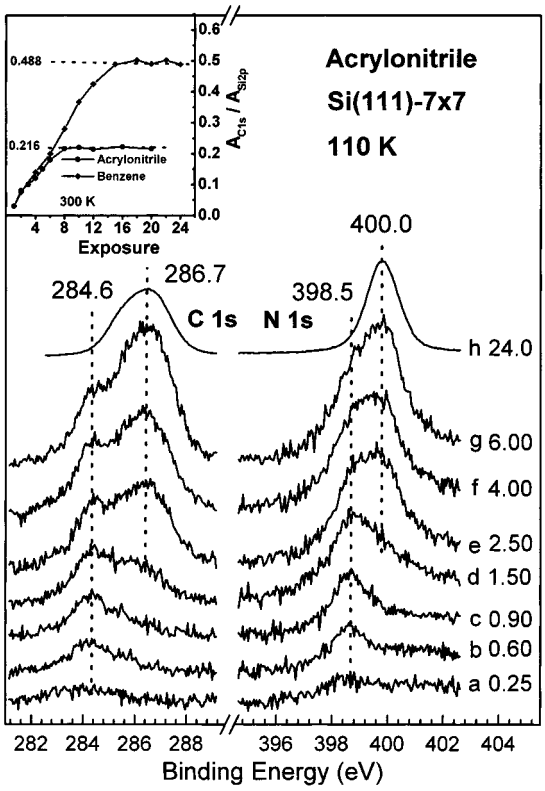

Figure 4. C 1s and N 1s XPS for acrylonitrile adsorbed on Si(111)-7 × 7 as a function of exposure at 110 K. The inset plots the XPS peak area ratios, A_{C1s} / A_{Si2p}, for acrylonitrile and benzene on Si(111)-7 × 7 as a function of exposure at 300 K, where the dotted lines represent the saturation of chemisorption.

red-shifts of 166 and 67 cm^{-1}, respectively, demonstrating the rehybridization of the C^3 atom from sp^2 to sp^3. These results clearly conclude that the C^3 atom directly binds to a Si surface dangling bond but not the C^2 atom. Similarly to chemisorbed acrylonitrile on Si(111)-7 × 7, the spectrum of chemisorbed acrylonitrile-2-d_1 (Figure 3b) also shows the characteristic vibrational modes of C═C═N at 2028, 1158, 868, and 615 cm^{-1}, further confirming our vibrational assignments for chemisorbed acrylonitrile on Si(111)-7 × 7. In addition, the peak at 1398 cm^{-1} in the spectrum of chemisorbed acrylonitrile (Figure 2d) does not display obvious shift in chemisorbed acrylonitrile-2-d_1 (1396 cm^{-1} in Figure 3b), attributable to the $-C^3H_2-$ scissor mode, but not $-C^2H(D)=$. Table 1 also lists the main vibrational frequencies of $Si-C^3H_2-C^2H=C^1=N-Si$ structure from our DFT calculations, unambiguously approving our assignments for chemisorbed acrylonitrile on Si(111)-7 × 7. The details of DFT theoretical modeling will be given in Section III E.

III B. X-ray Photoelectron Spectroscopy. Figure 4 shows the C 1s and N 1s XPS spectra of acrylonitrile adsorbed on Si(111)-7 × 7 at 110 K as a function of exposure. For acrylonitrile exposures <2.5 L, a doublet of C 1s photoemission feature centered at 284.6 eV (fwhm of ∼2.6 eV) and a nearly symmetrical N 1s peak at 398.5 eV are observed, ascribable to chemisorbed acrylonitrile. When increasing the exposure, the C 1s peak at 286.7 eV and N 1s peak at 400.0 eV corresponding to physisorbed molecules gradually increase and dominate the XPS spectra at exposures higher than 6 L. The photoemission from chemisorbed acrylonitrile is completely attenuated at an exposure of ∼24 L.

The area ratio A_{C1s}/A_{Si2p} is plotted as a function of acrylonitrile exposure in the inset of Figure 4. The value for each point was obtained by averaging three separate measurements to reduce possible errors. A_{C1s} is the C 1s peak area of chemisorbed acrylonitrile at 300 K. The saturation of the A_{C1s}/A_{Si2p} ratio indicates the completion of chemisorption. To estimate its absolute saturation coverage, XPS measurements for acrylonitrile-saturated Si(111)-7 × 7 are compared to those of chemisorbed benzene. The saturation coverage of benzene, $\theta_{benzene}$, was known to be ∼0.10, defined as the ratio of the reacted adatoms to the 49 silicon atoms in a unit cell.[28] This value becomes ∼0.42 if the coverage is defined as the ratio between the reacted adatoms and the total adatoms on Si(111)-7 × 7.

The inset of Figure 4 presents the ratio of A_{C1s}/A_{Si2p} as a function of acrylonitrile exposure at room temperature, giving ∼0.216 for the saturated chemisorption monolayer. A saturation ratio of 0.488 was also found for chemisorbed benzene, which corresponds to an absolute coverage of 0.42.[28] After considering the numbers of carbon atoms in these two molecules, the saturation coverage, $\theta_{acrylonitrile}$, is estimated to be around ∼0.38 [= 0.42 × 0.216/0.488 × 6/3]. This value reckoned with XPS is consistent with the statistical result from our STM images of

(26) Schwartz, M. P.; Ellison, M. D.; Coulter, S. K.; Hovis, J. S.; Hamers, R. J. *J. Am. Chem. Soc.* **2000**, *122*, 8529−8538.
(27) Hamaguchi, K.; Machida, S.; Nagao, M.; Yasui, F.; Mukai, K.; Yamashita, Y.; Yoshinobu, J.; Kato, H. S.; Okuyama, H.; Kawai, M.; Sato, T.; Iwatsuki, M. *J. Phys. Chem. B* **2001**, *105*, 3718−3723.
(28) Taguchi, Y.; Fujisawa, M.; Nishijima, M. *Chem. Phys. Lett.* **1991**, *178*, 363−368.

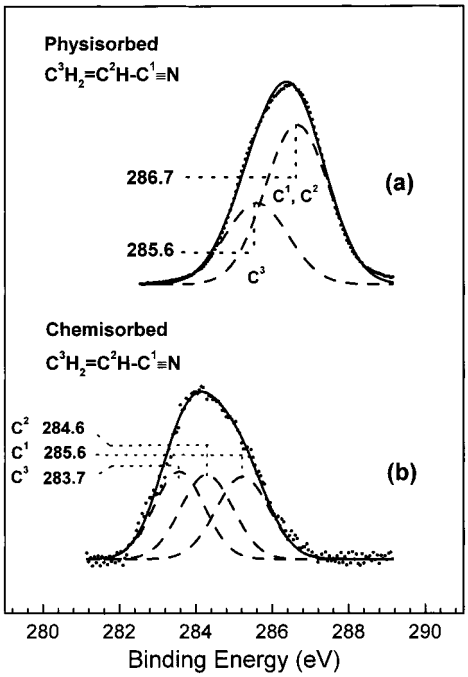

Figure 5. Fitted C 1s spectra for physisorbed and saturated chemisorbed acrylonitrile on Si(111)-7 × 7. For fabricating a saturated chemisorpiton acrylonitrile monolayer on the Si(111)-7 × 7, a sample was preexposed to 12 langmuirs of acrylonitrile at 110 K and then annealed to 300 K to drive all of the physisorbed molecules away and leave only the chemisorbed acrylonitrile on the surface.

a saturated acrylonitrile monolayer on Si(111)-7 × 7 at 300 K, to be described in Section III D.

Figure 5 shows the fitted C 1s XPS spectra for physisorbed and chemisorbed $C^3H_2{=}C^2H{-}C^1{\equiv}N$ on Si(111)-7 × 7. The C 1s spectrum of physisorbed molecules is deconvoluted into two peaks centered at 285.6 and 286.7 eV with equal fwhm and an area ratio of 1:2.05 (Figure 5a), in excellent accordance with the results of physisorbed acrylonitrile on Cu(100), Pt(111), and Au(111).[29,30] It is also consistent with the DFT calculation results obtained by Crispin et al.,[30] showing that the BEs of C^1 and C^2 separated by 0.19 eV are ~1.1 eV higher than that of the C^3 atom. Resolving the C 1s BE difference of ~0.2 eV between C^1 and C^2 by further deconvolution was not attempted because of the limitation of our XPS resolution. Thus, the peak at 286.7 eV can be attributed to the C^1 and C^2, whereas the other at 285.6 eV can be attributed to the C^3 of physisorbed molecules.[29,30]

The XPS results for chemisorbed acrylonitrile are shown in Figure 5b. The C 1s spectrum of chemisorbed molecules was fitted into three peaks at 283.7, 284.6, and 285.6 eV with the same fwhm and an area ratio of 1:1.05:1.08, respectively. This result suggests that there are three chemically inequivalent carbon atoms in the chemisorbed molecule. The significant change in the C 1s spectrum upon chemisorption shows a large difference in electronic structure between the chemisorbed and physisorbed acrylonitrile on Si(111)-7 × 7. A detailed discussion of this difference and the assignments of the three peaks in Figure 5b will be presented in Section IV.

III C. Ultraviolet Photoelectron Spectroscopy. The acrylonitrile molecule is planar in its ground electronic state and is of C_s symmetry. The photoemission from the valence band of gaseous acrylonitrile molecules was extensively investigated with high-resolution He I photoelectron spectroscopy and He* penning ionization techniques.[31−33] Lake and Thompson [31] reported seven ionization energy levels. The first is located at 10.91 eV, assigned to the ionization from the π orbital of the vinyl group.[33] The second at 12.36 eV is associated with the photoemission of electrons located at the π_{CN} (12a′) orbital of the cyano group.[30] The narrow and intense peak at 13.04 eV is attributable to the emission of valence electrons from the 1a″ molecular orbital with a mixed character of conjugated π'_{CN} and $\pi_{C=C}$. The other four bands at 13.53, 14.44, 16.17, and 17.62 eV are attributable to σ_{CN}, π_{CH_2}, σ_{C-C}, and C_{2s} (CN), respectively.

Table 2. Peak Assignments of Valence Band Spectral Features for Valence Band Spectrum of Physisorbed Acrylonitrile (110 K) and Difference Spectrum of Chemisorbed Molecules (300 K) on Si(111)-7 × 7[a]

	gas phase		physisorbed acrylonitrile		chemisorbed acrylonitrile	
MO type	orbital	av	peak	energy	peak	energy
$\pi_{C=C}$	2a″ (10.91)	10.91	A	6.06	A′	3.00
$\pi_{C\equiv N}$	12a′ (12.36)				B_1'	7.50[c]
$\pi_{C=C}, \pi'_{C\equiv N}$	1a″ (13.04)	13.04[b]	B	8.24[c]		
σ_{CN}	11a′ (13.53)				B_2'	8.60[c]
π_{CH_2}	10a′ (14.44)					
σ_{C-C}	9a′ (16.17)	16.17	C	11.30	C′	11.30

[a] The ionization energies of the gas-phase molecular orbitals are shown in parenthesis. All energy is in eV. [b] Average value of energy corresponding to $\pi'_{C\equiv N}$ (12a′), π'' (1a″) (C=C and C≡N), σ_{CN} , and π_{CH_2}. [c] This value is the energy of the central point of its corresponding peak.

Previous valence band spectra of acrylonitrile have shown that π_{CN} splits into two levels, π_{CN} (12a′) and π'_{CN} (1a″), with an energy separation of 0.68 eV (Table 2).[34] The π'_{CN} (1a″) of the C≡N group is perpendicular to the molecular plane, forming a conjugated orbital with $\pi_{C=C}$ (1a″). The other π_{CN} (12a′) is in the molecular plane. In view of the fact that the inductive effect of the C≡N group is larger than the conjugation effect,[34] the induction of the C≡N group stabilizes the $\pi_{C=C}$ (2a″) orbital (its ionization energy is 10.91 eV instead of 10.51 eV for $CH_2{=}CH_2$). The π'_{CN} (1a″) is destabilized as a result of the increase in electron density and has an ionization energy lower than expected if only considering a pure conjugation effect.

Figure 6 presents the He II photoelectron spectra of acrylonitrile on Si(111)-7 × 7 as a function of exposure at 110 K. The inset (Figure 6) shows that increasing exposure leads to the attenuation of dangling bond surface states and a total quenching at ~2 L of acrylonitrile, correlating well with the saturation of chemisorption revealed by XPS. Upon 6 L of exposure, the photoemission from the valence bands of chemisorbed molecules is completely screened by the physisorbed multilayer, resulting in four dominant features at 6.06 (A), 8.24 (B), 11.30 (C), and 12.70 eV (D) below E_F. It can be seen from Table 2 that for physisorbed acrylonitrile, the energy separations between two successive levels agree well with those of gas-

(29) Korzeniewski, C.; Pons, S. *J. Vac. Sci. Technol. B* **1985**, *3*, 1421−1426.
(30) Crispin, X.; Bureau, C.; Geskin, V. M.; Lazzaroni, R.; Salaneck, W. R.; Bredas, J. L. *J. Chem. Phys.* **1999,** *111*, 3237−3251.
(31) Lake, R. F.; Thompson, H. *Proc. R. Soc. London, Ser. A* **1970**, *317*, 187−195.
(32) Ohno, K.; Harada, Y.; Imai, K.; Matsumoto, S. *J. Phys. Chem.* **1984**, *88*, 206−209.
(33) Delwiche, J.; Gochel-Dupis, M.; Collin, J. E.; Heinesch, J. *J. Electron. Spectrosc. Relat. Phenom.* **1993**, *66*, 65−74.
(34) Ohno, M.; Niessen, W. V.; Gochel-Dupuis, M.; Delwiche, J.; Heinesch, J. *J. Electron. Spectrosc. Relat. Phenom.* **1996**, *77*, 149−154.

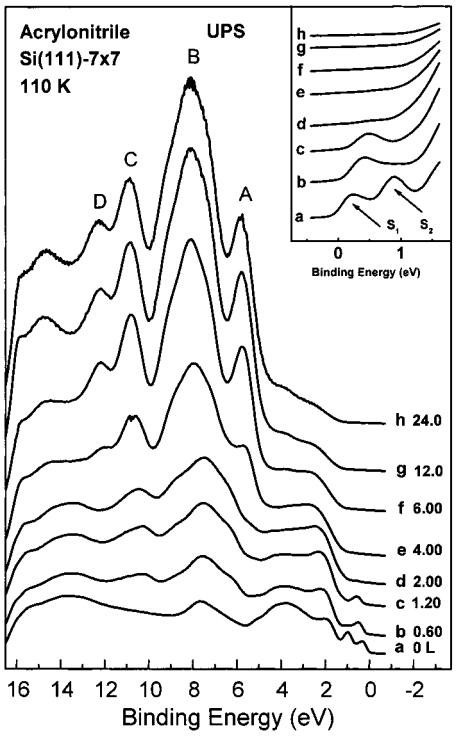

Figure 6. Valence-band spectra of acrylontirle on Si(111)-7 × 7 as a function of exposure at 110 K. The inset shows the influence of acrylonitrile exposure on the dangling bond surface states of the Si(111)-7 × 7.

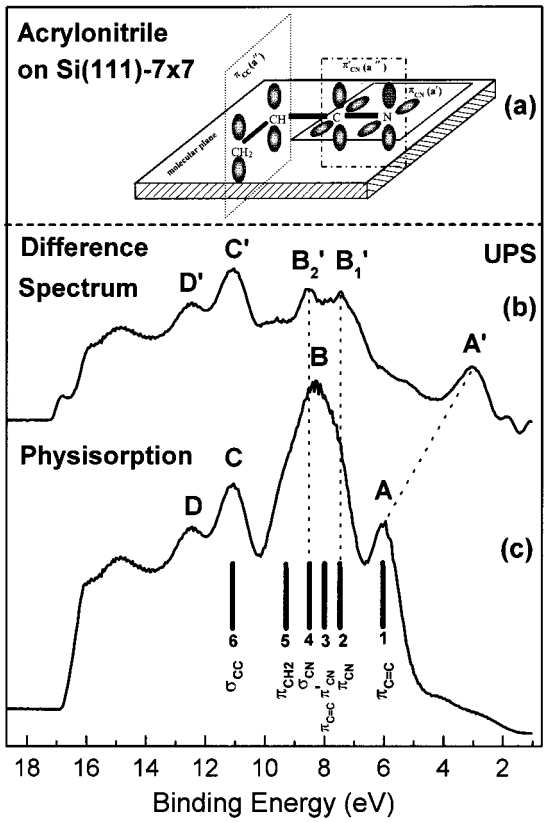

Figure 7. Valence band spectra of physisorbed acrylonitrile and the difference spectrum of the saturated chemisorption molecules on Si(111)-7 × 7. The top panel (a) is the schematic diagram of acrylonitrile molecular orbitals.

phase UPS.[31−35] The peak-broadening and spectrum shift in energy are due to the solid-state effects and changing in reference levels. Thus, the four bands of A, B, C, and D observed for physisorbed molecules in our experiment can be assigned to $\pi_{C=C}$ (2a″), [π_{CN} (12a′) + $\pi_{C=C}$ (1a″) + $\pi'_{C\equiv N}$ (1a″) + σ_{CN} (11a′) + π_{CH_2}], σ_{C-C}, and C_{2s} of CN, respectively.

The UPS of chemisorbed acrylonitrile was obtained after annealing the sample predosed to 12 L of acrylonitrile at 110−300 K to drive away all physisorbed molecules. Figure 7 compares the UPS features between physisorbed and chemisorbed acrylonitrile. The schematic diagram of gaseous acrylonitrile molecular orbitals is presented in Figure 7a. Because σ_{C-C} (peak C) does not take part in the interaction with the Si surface, its intensity was taken as a reference to estimate changes in the relative intensities for other orbitals.

In the UPS spectrum of physisorbed acrylonitrile, peak B shown in Figure 7c is nearly symmetrical and sharp and is assigned to the combination of π_{CH_2}, σ_{CN} (11a′), π'_{CN} (1a″), $\pi_{C=C}$ (1a″), and π_{CN} (12a′). However, in the valence band spectrum of chemisorbed molecules, the photoemission intensity of peak B′ is significantly reduced, splitting into two peaks (B_1' and B_2' in Figure 7b) located at 7.5 and 8.6 eV, respectively. This reduction in intensity suggests that some constituent orbitals of peak B observed for physisorbed acrylonitrile directly participate in chemisorption, which is consistent with the disappearance of the dangling bond surface states (the inset of Figure 6). In addition, a new photoemission peak at 3.0 eV can be clearly resolved for chemisorbed acrylonitrile. The detailed assignment of UPS features will be discussed in Section IV.

III D. Scanning Tunneling Microscopy. To further elucidate the nature of acrylonitrile chemisorbed on Si(111)-7 × 7, STM was employed to investigate its site selectivity and spatial distribution. Figure 8a is the STM constant current topographs (CCTs) of a clean Si(111)-7 × 7 surface with a defect density of < 0.5%, estimated by counting an area containing about one thousand adatoms. Figure 8c is the in situ STM observation upon initial acrylonitrile adsorption for the same region as that of Figure 8b. The adatoms labeled as A, B, and C are used to identify the locations of other adatoms before and upon chemisorption. Compared to the clean Si(111)-7 × 7 surface (Figure 8b), two center adatoms in two subunits (highlighted with green cycles in Figure 8b,c) disappear upon initial chemisorption. The darkened features presented in Figure 8c indicate the disappearance of the dangling bond surface states and the elimination of electron density at these sites as a result of the chemisorption. This is consistent with the gradual attenuation of the photoemission signal from dangling bond surface states of Si(111)-7 × 7 with an increasing exposure of acrylonitrile detected by UPS. There is no bias dependence observed in STM studies, suggesting that the chemisorbed acrylonitrile and reacted adatoms do not have molecular orbitals close to Fermi level (E_F). The distinct formation of darkened sites whose number increases with exposure was also observed for the chemisorption of other small molecules, including C_2H_2,[36] C_2H_4,[37] C_4H_4S,[38] C_6H_6,[39] C_6H_6Cl,[40] H_2O,[41] and NH_3[42]

(35) Perreau, J.; Reyuaud, C.; Lecayon, G.; Ellinger, Y. *J. Phys. B*, **1986**, *19*, 1497−1505.
(36) Yoshinobu, J.; Fukushi, D.; Uda, M.; Nomura, E.; Aono, M. *Phys. Rev. B.* **1992**, *46*, 9520−9524.
(37) Yoshinobu, J.; Tasuda, T.; Onchi, M.; Nishijima, M. *Chem. Phys. Lett.* **1986**, *130*, 170−174.
(38) Cao, Y.; Yong, K. S.; Wang, Z. H.; Deng, J. F.; Lai, Y. H.; Xu, G. Q. *J. Chem. Phys.* **2001**, *115*, 3287−3296.
(39) Wolkow, R. A.; Moffatt, D. J. *J. Chem. Phys.* **1995**, *103*, 10696−10700.

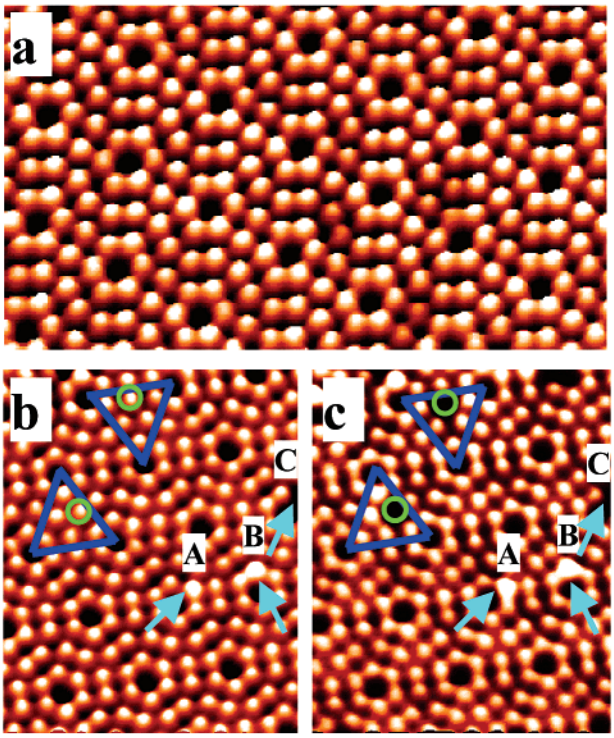

Figure 8. STM constant current topographs (CCTs) of clean (a and b) and acrylonitrile-exposed (c) Si(111)-7 × 7 at 300 K. The marks A, B, and C in parts b and c are used to identify the locations of other adatoms upon in situ dosing.

on Si(111)-7 × 7. In all of these systems, the darkening of adatoms in the STM images was attributed to the consumption of dangling bonds of adatoms as a result of the new surface−adsorbate bond formation.

A statistical counting of darkened dangling bond sites can provide information on the spatial selectivity for arcylonitrile chemisorption. The inspection of several different exposures of acrylonitrile manifests the preferential adsorption on the center adatom sites of faulted halves. Statistical results also show that the center-adatoms have a reactivity about two times that of the corner adatoms. In addition, the adatoms in the faulted subunit react preferentially over those in unfaulted subunits at a ratio of ∼2.2:1 at low coverages. At saturated chemisorption (Figure 9), substantial adsorption also occurs on unfaulted halves. However, the preference of center adatoms over the corner adatom sites is still evident. The higher selectivity of acrylonitrile binding to the adatom sites on the faulted half of a Si(111)-7 × 7 unit cell can be understood when considering the higher electrophilicity of the faulted subunits[43] and a smaller strain for molecules binding on the center-adatom.[42] The STM images containing ∼100 unit cells show that the saturation coverage is ∼0.42, defined as the ratio of reacted adatoms to the total adatoms, which is in good agreement with the value of ∼0.38 measured by XPS (Section III B). This value approximately corresponds to 5 acrylonitrile molecules/unit cell. Furthermore, the careful examination of the STM images shows that the maximum number of adatoms involved in acrylonitrile chemisorption for every faulted or unfaulted half unit cell is three, equal to the number of rest atoms. Thus, it is reasonable to deduce that every acrylonitrile molecule binds with the neighboring adatom−rest atom pair.

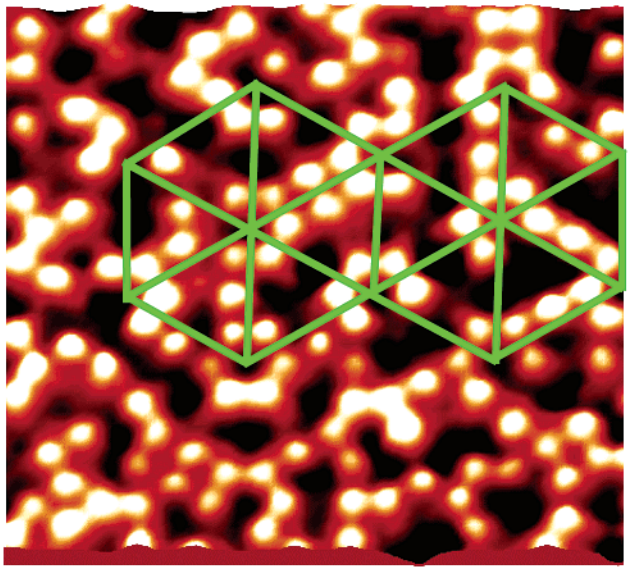

Figure 9. STM constant current topographs (CCTs) of saturated chemisorption acrylonitrile on Si(111)-7 × 7 at 300 K.

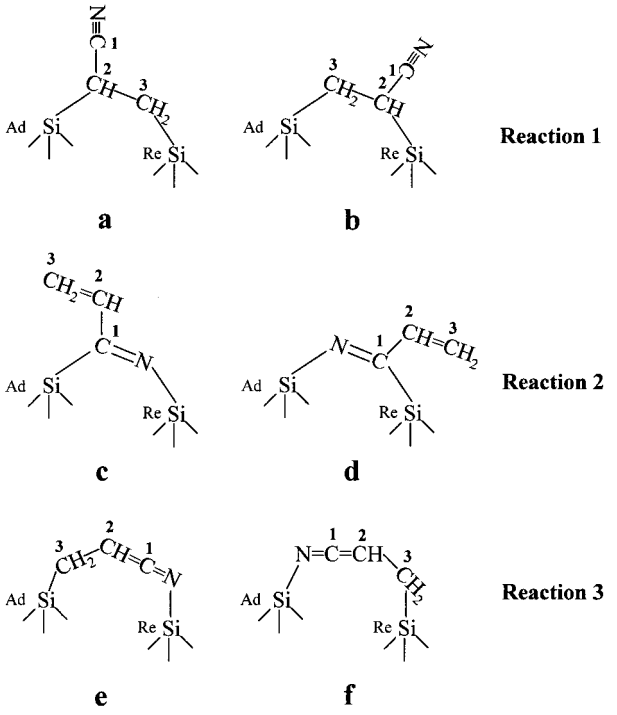

Figure 10. Schematic diagrams of six possible addition products corresponding to three possible reaction pathways.

III E. DFT Calculations. Acrylonitrile contains C═C and C≡N bonds as two reactive functional groups in a conjugated arrangement. If the concept of *di-σ* attachment modes is considered, there are altogether six possible configurations for chemisorbed acrylonitrile: four [2 + 2]-like cycloadducts (Figure 10a−d) and two [4 + 2]-like addition products (Figure 10e,f). A theoretical investigation was carried out to further understand the reactivity determined in our experiments.

(40) Chen, X. H.; Kong, Q.; Polanyi, J. C.; Rogers, D.; So, S. *Surf. Sci.* **1995**, *340*, 224−230.
(41) Avouris, P.; Lyo, I. W. *Surf. Sci.* **1991**, *242*, 1−11.
(42) Avouris, Ph.; Wolkow, R. A. *Phys. Rev. B* **1989**, *39*, 5091−5100.
(43) Brommer, K. D.; Galvan, M.; Dal Pino, A., Jr.; Joannopoulos, J. D. *Surf. Sci.* **1994**, *314*, 57−70.

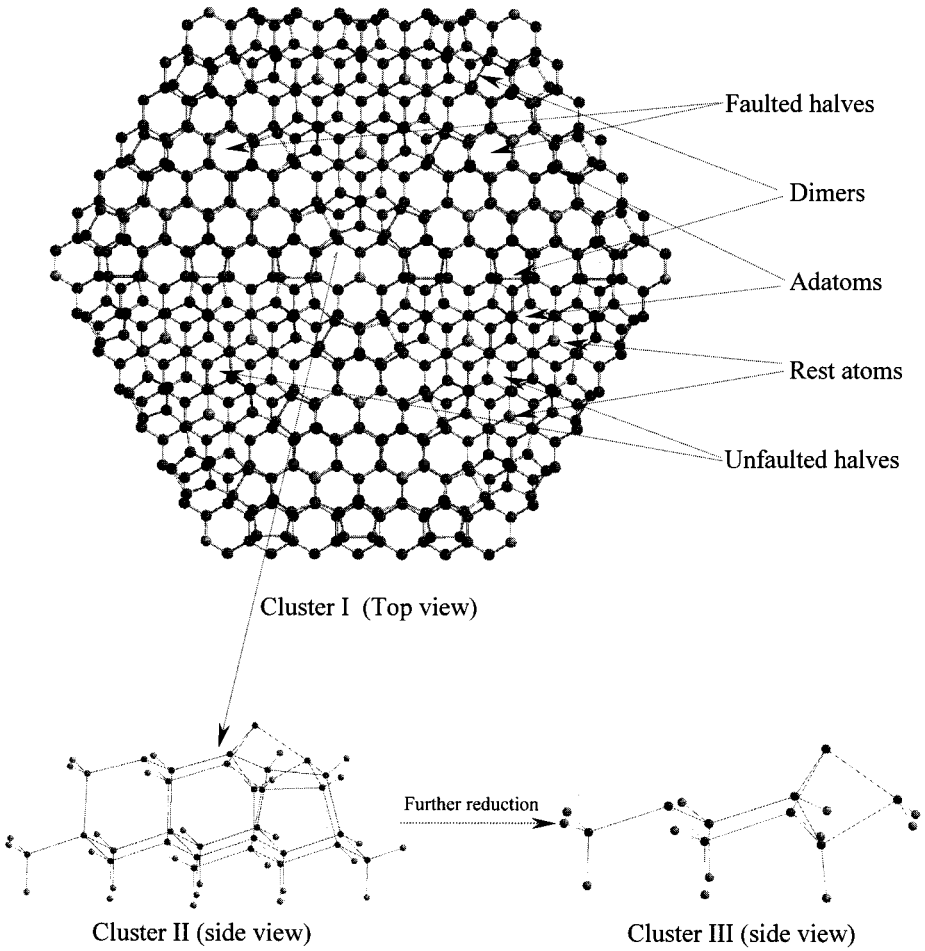

Figure 11. Large cluster of the top five silicon layers constructed on the basis of the DAS model to present three Si(111)-7 × 7 unit cells surrounding a corner hole. It (cluster I) has 973 atoms, including the capping H atoms (not displayed for clarity). Clusters II ($Si_{30}H_{28}$) and III (Si_9H_{12}) are reduced from cluster I.

As shown in the bottom-left panel of Figure 11, cluster model II ($Si_{30}H_{28}$) was cut from the central part of MMFF94[44] optimized cluster I (the top panel of Figure 11), where the precision of atomic positions suffers the least from boundary effects. It contains an adatom and an adjacent rest atom from an unfaulted subunit, serving as a "*di-σ*" binding site for the attachment of one acrylonitrile molecule. Capping H atoms at the cluster boundaries are kept frozen. Silicon atoms in the bottom double layers are placed at bulk lattice positions prior to the geometry optimization process, with each Si−Si bond length set to 2.3517 Å and all bond angles adjusted to 109.4712°. Cluster III (Si_9H_{12}) was obtained from further reduction of cluster II. Similarly, all capping H atoms were frozen during geometry optimization. Clusters corresponding to the six possible binding models were constructed by $C^3H_2{=}C^2H{-}C^1{\equiv}N$ adsorption onto the mother cluster (cluster III of Figure 11) via [2 + 2]-like reactions through vinyl or cyano group and [4 + 2]-like cycloaddition with the two terminal atoms of the acrylonitrile molecule. Clusters I, II, and III were used in successful prediction of the adsorption energy of benzene on Si(111)-7 × 7.[45]

Calculations were performed using the SPARTAN package.[46] The formation heats of chemisorbed configurations were calculated at the DFT theory level using the perturbative Beck−Perdew functional (*p*BP86) in conjugation with a basis set of DN** (comparable to 6-31 G**).[46] Geometric optimizations were conducted under SPARTAN default criteria. Adsorption energy, synonymous with formation heat, is quoted here as the difference between the energy of the adsorbate/substrate complex and the total sum of the substrate and gaseous molecule. Figure 12 presents the six optimized geometries of the local minimums for the C_3H_3N/Si_9H_{12} model system. The adsorption energies are given in Table 3. The calculation result reveals that the [4 + 2]-like cycloadditions is thermodynamically favored when compared to the [2 + 2]-like reactions. Cluster $[4 + 2]_1$ (Figures 10e and 12a) is seen to be the most stable, where the N and C^3 atoms are linked to the rest atom and adatom, respectively, forming a $H_3C^3{-}C^2H{=}C^1{=}NH$-like structure. This process is exothermic by 60.8 kcal mol^{-1}. In addition, the calculated vibrational frequencies (Table 1) of the most stable intermediate, cluster $[4 + 2]_1$ (Figure 12a), are very consistent with the experimental vibrational spectrum.

IV. Discussion

There are various possible ways for acrylonitrile adsorption on Si(111)-7 × 7. One way is to undergo an end-on binding

(44) Halgren, T. A. *J. Comput. Chem.* **1996**, *17*, 490−519.
(45) Wang, Z. H.;. Cao, Y.; Xu, G. Q. *Chem. Phys. Lett.* **2001**, *338*, 7−13.
(46) Hehre, W. J.; Yu, J.; Klunzinger, P. E.; Lou, L. *A Brief Guide to Molecular Mechanics and Quantum Chemical Calculation*, Wavefunction: Irvine, CA, 1998.

Table 3. Adsorption Energies of the Local Minimums in the C_3H_3N/Si_9H_{12} Model System from *p*BP/DN

	functional group					
	$C^3H_2{=}C^2H$	$C^3H_2{=}C^2H$	$C^1{\equiv}N$	$C^1{\equiv}N$	$C^3H_2{=}C^2H{-}C^1{\equiv}N$	$C^3H_2{=}C^2H{-}C^1{\equiv}N$
reaction model	[2 + 2]	[2 + 2]	[2 + 2]	[2 + 2]	[4 + 2]	[4 + 2]
termination[a]	$(Si_a)C^3H_2C^2H(Si_r)$	$(Si_r)C^3H_2C^2H(Si_a)$	$(Si_a)C^1{=}N(Si_r)$	$(Si_r)C^1{=}N(Si_a)$	$(Si_a)C^3H_2C^2H{=}C^1{=}N(Si_r)$	$(Si_r)C^3H_2C^2H{=}C^1{=}N(Si_a)$
adsorption energy[b]	−35.2	−33.9	−30.3	−29.4	−60.8	−54.5

[a] Si_a, adatom; Si_r, rest atom. [b] Adsorption energy: $\Delta E = E(C_3H_3N/Si_9H_{12}) - E(Si_9H_{12}) - E(C_3H_3N)$. All energies are in kcal mol^{-1}.

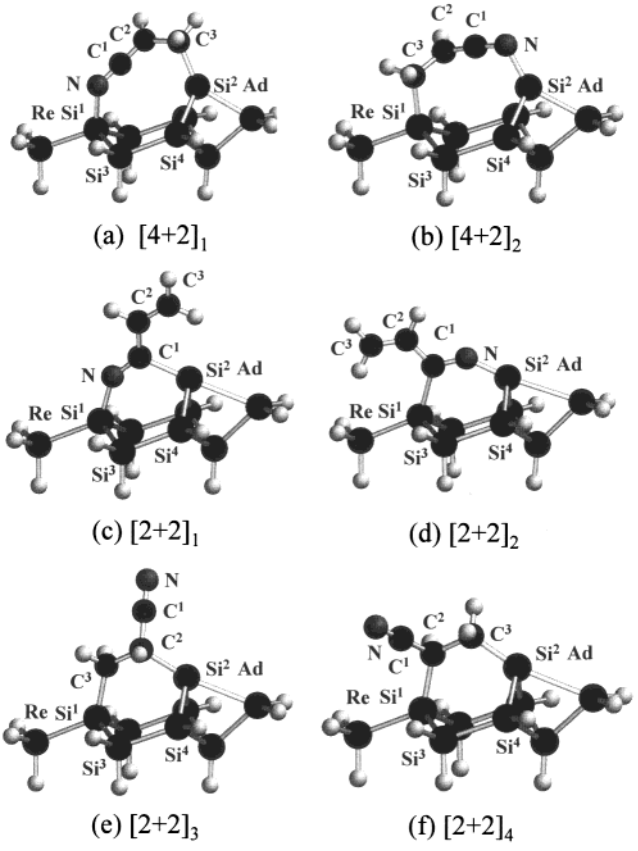

Figure 12. Optimized C_3H_3N/Si_9H_{12} clusters corresponding to the six possible attachment models through [4 + 2]-like addition reactions via the two terminal atoms of $C^3H_2{=}C^2H{-}C^1{\equiv}N$ and [2 + 2]-like cycloadditions via a C═C vinyl or cyano group.

mechanism in which the lone pair on the nitrogen atom binds with the Si surface dangling bond, similarly to the adsorption of acetonitrile on Cu(100).[47] Since the interaction is expected to be weak, the resulting configuration of $C^3H_2{=}C^2H{-}C^1{\equiv}N{\cdots}Si$ basically preserves the structure of the acrylonitrile molecule. The vibrational features of the end-on bonded acrylonitrile would be similar to those of physisorbed molecules. In addition, there are three possible pathways for the covalent attachment (six configurations) of acrylonitrile on Si(111)-7 × 7, schematically presented in Figure 10. The [2 + 2]-like cycloaddition through the vinyl group forms a surface intermediate of $(Si)C^3H_2{-}C^2H(Si){-}C^1{\equiv}N$ (Figure 10a, b). In this reaction product, both C^2 and C^3 atoms rehybridize from sp^2 into sp^3, and the $C^1{\equiv}N$ group is retained. One would expect to detect only the (sp^3) C−H stretching mode at <3000 cm^{-1}, together with the $C^1{\equiv}N$ stretching vibration around 2239 cm^{-1}. The [2 + 2]-like addition through the cyano group to a neighboring adatom−rest atom pair gives a chemisorbed species of $C^3H_2{=}C^2H{-}(Si)C^1{=}N(Si)$ (Figure 10c,d) with a $C^3{=}C^2{-}C^1{=}N$ conjugated structure. In these cycloadducts, the retention of $C^3H_2{=}C^2H{-}$ is expected to produce (sp^2) C−H stretching features similar to those for physisorbed molecules (two separate peaks at ∼3102 and ∼3032 cm^{-1}), together with the absence of $C^1{\equiv}N$ stretching around 2239 cm^{-1} and the appearance of $C^1{=}N$ stretching at 1550−1700 cm^{-1}. The [4 + 2]-like reactions involving the C^3 and N atoms of $C^3H_2{=}C^2H{-}C^1{\equiv}N$ form cycloadducts (Figure 10e,f) containing a $(Si)C^3H_2{-}C^2H{=}C^1{=}N(Si)$ skeleton. In this reaction, only the C^3 atom rehybridizes from sp^2 into sp^3. The breakage of the conjugated $\pi_{C^3=C^2}$ and π'_{CN} bonds results in the formation of a new $\pi_{C^2=C^1}$. The $(sp^3)C^3{-}H$ of $-C^3H_2-$ and $(sp^2)C^2{-}H$ of $-C^2H{=}$ stretching modes are expected to coexist in the vibration features of chemisorbed species. Additionally, the disappearance of the C≡N vibrational feature should be accompanied by the observation of the vibrational modes of the cumulative double bond C═C═N.

In our HREELS studies of chemisorbed molecules, the coexistence of $(sp^2)C^2{-}H$ at 3034 cm^{-1} and $(sp^3)C^3{-}H$ at 2938 cm^{-1} coupled with the absence of the $C^1{\equiv}N$ stretching at ∼2239 cm^{-1} was observed, showing the simultaneous involvement of the $C^3{=}C^2$ and $C^1{\equiv}N$ groups in the interaction with the Si surface. This result clearly rules out the possibility of [2 + 2]-like cycloaddition occurring only through the $C^3{=}C^2$ group or the $C^1{\equiv}N$ group. In addition, it excludes the weak end-on binding mode through the interaction of the lone pair on the nitrogen atom with the surface dangling bond.

In fact, our results are consistent with the [4 + 2]-like cycloaddition reaction mechanism, forming a product containing a $-C^3H_2{-}C^2H{=}C^1{=}N-$ skeleton (Figure 10e,f). In this structure, the coexistence of $(sp^3)C^3{-}H$ and $(sp^2)C^2{-}H$ is expected, together with the conversion of $C^1{\equiv}N$ to $C^1{=}N$ upon cycloaddition. The characteristic $C^2{=}C^1{=}N$ skeleton of the surface intermediate is further confirmed by the detection of its asymmetic stretching mode at 2032 cm^{-1}, together with its symmetric stretching, torsion, and bend modes at 1167, 835, and 607 cm^{-1}, respectively. Hence, the vibrational characteristics allow us to conclude that acrylonitrile covalently bonds to the Si surface principally through breaking *both* $\pi_{C=C}$ and π'_{CN} bonds to react with the dangling bonds located on the adjacent adatom−rest atom pair via the [4 + 2]-like process.

The changes in the valence band photoemission observed in our UPS studies are in good agreement with the [4 + 2]-like cycloaddition reaction. For the physisorbed multilayer, the bands at 6.06 (A) and 8.24 eV (B) are related to $\pi_{C=C}$ (2a″) and [π_{CN} (12a′) + $\pi_{C=C}$ (1a″) + $\pi'_{C\equiv N}$ (1a″) + σ_{CN} (11a′) + π_{CH2}], respectively. The chemisorption involves the breakage of the conjugated π'_{CN} (1a″) and $\pi_{C=C}$ (1a″) bonds, forming a new $\pi_{C=C}$ bond between the C^1 and C^2 atoms. In addition, the π_{CH_2} is expected to disappear as a result of the rehybridization of

(47) Sexton, B. A.; Avery, N. R. *Surf. Sci.* **1983**, *129*, 21−36.

Table 4. Fitted Result of XPS Spectra for Chemisorbed and Physisorbed Acrylonitrile on Si(111)-7 × 7[a]

C^3H_2═C^2H–C^1N	physisorption	chemisorption	chemical shift	rehybridization
N	400.0	398.5	1.5	$sp-sp^2$
C^1	~286.7	~285.6	~1.1	sp−sp
C^2	~286.7	~284.6	~2.1	sp^2-sp^2
C^3	285.6	~283.7	~1.9	sp^2-sp^3

[a] All energies are in eV

the C^3 atom from sp^2 into sp^3 after this cycloaddition, but the unconjugated π_{CN} is retained. Compared to physisorbed molecules, a significant reduction in photoemission intensity is indeed observed for the B′ band in the UPS spectrum of chemisorbed acrylonitrile (Figure 7b). The constituent peaks, B_1' and B_2', of the B′ band can assigned to the π_{CN} and σ_{CN} orbitals, respectively, existing in chemisorption species of (Si)$C^3H_2-C^2H$═C^1═N(Si). The intensity observed at 3.0 eV (peak A′) can be attributed to the $\pi_{C=C}$ of the newly formed $-C^2H$═C^1═ in chemisorption. Peak A′ displays a large downshift of ~3.0 eV referenced to peak A of physisorbed molecules. Compared to the conjugated $\pi_{C=C}$ (1a″) of physisorbed acrylonitrile, the newly formed $-C^2H$═C^1═ in the chemisorbed species is not conjugated and induced by the CN group, resulting in a higher electron density and a lower binding energy for its $\pi_{C=C}$.

The deconvoluted C 1s XPS data obtained for chemisorbed acrylonitrile (Figure 5b) can be reasonably explained by the [4 + 2]-like cycloaddition. The three constituent C 1s peaks at 285.6, 284.6, and 283.7 eV can be assigned to the C^1, C^2, and C^3 atoms of the reaction adduct (Si)$C^3H_2-C^2H$═C^1═N(Si). Table 4 lists the detailed assignment of C 1s and N 1s core levels for physisorbed and chemisorbed acrylonitrile on Si(111)-7 × 7. This assignment is justified and consistent if comparison with previous studies is made. The C^3 atom with sp^3 hybridization in chemisorbed acrylonitrile is chemically analogous to the C atom of chemisorbed ethylene on Si(100),[48] giving similar binding energies for C 1s photoemission. Our assignment of the C 1s at 284.6 eV to the C^2 atom is consistent with the C 1s value of the remaining C═C bond in chemisorbed 1,5-cyclooctadiene on Si(100).[49] The C^1 atom has the highest C 1s BE at 285.6 eV as a result of its sp hybridization. Although the C^1 atom retains the same sp hybridization upon chemisorption, its C 1s BE downshifts by ~1.1 eV referenced to the value of physisorbed acrylonitrile. The rehybridization of the nitrogen atom and its bonding to a Si atom with a much lower electronegativity (Pauling electronegativity = 1.90) reduce the electronic polarization in the C^1═N. Thus, compared to physisorbed acrylonitrile, a higher electron density is expected at the C^1 atom, leading to a lower C 1s BE of the C^1 atom. Although the C^2 atom in chemisorbed and physisorbed acrylonitrile has the same sp^2 hybridization, a dramatic downshift of ~2.2 eV is detected upon chemisorption. This can be understood if considering the strong inductive effect of the C^1≡N group to the C^3═C^2 group in physisorbed molecules, decreasing the electron density at the C^2 atom. However, this effect is not present for the chemisorption product, thereby resulting in a higher electronic density around the C^2 atom when compared to physisored molecules.

The reactivity of acrylonitrile on Si(111)-7 × 7 can also be rationalized from the combined effects of the *polarities* of organic groups and reactive sites (the adjacent adatom−rest atom) and the *spatial arrangements* of the acrylonitrile molecule and the neighboring adatom−rest atom pair on the surface. As was well-documented, the reactive sticking probabilities of cyclopentene on Si(100) (1.0),[50] Ge(100) (0.1),[51] and C(100) (0.001)[52] closely correlate with the extent of surface dimer buckling. The dimers on Si(100) and Ge(100) are experimentally and theoretically shown to be buckled.[53−56] However, no buckling dimers are present on C(100).[54−56] The electron transfer from the "down" atom to the "up" atom results in the polarization of Si═Si and Ge═Ge dimers, making the buckled-down atom electrophilic and buckled-up atom nucleophilic.[52,53] These results clearly demonstrate that polarization in surface dimers significantly enhances their reactivity with the C═C group of organic molecules.[52] A similar approach may be also employed to understand the selectivity of reactive channels in acrylonitrile adsorption on Si(111)-7 × 7. In the three reactive groups including C^3═C^2, C^1≡N, and C^3═C^2-C^1≡N, the larger polarities of the C^1≡N group and C^3═C^2-C^1≡N skeleton make them *both* electrophilic and nucleophilic, as compared to the C^3═C^2 group. On the other hand, the adjacent adatom−rest atom pair can also be considered as a strong dipole, because each rest atom has a formal charge of −1 and every adatom has an electron occupancy of only 5/12 instead of 1 electron, leading to a formal charge of +7/12 (~+0.58).[57] Thus, for the chemisorption of acrylonitrile on Si(111)-7 × 7, lower transition states are expected for the cycloaddition between the polar C^3═C^2-C^1≡N (or C^1≡N) and the neighboring adatom−rest atom pairs. On the other hand, the spatial distribution of reactants, including the arrangement of the adjacent adatom−rest atom pair and the dimension of organic reactive groups, is also an important factor to influence the competitive reactions. The C^3-C^2 distance in the (Si)$C^3H_2-C^2H$(Si)− or the C^1═N bond length in $-C^1$(Si)═N(Si) formed through the [2 + 2]-like addition of C^3═C^2 or C^1≡N groups, respectively, is much smaller than 4.5 Å, thereby resulting in a large strain in the products. However, the dimension of the (Si)$C^3H_2-C^2H$═C^1═N(Si) formed via the [4 + 2]-like addition mechanism matches well the separation of 4.5 Å between the adatom and its adjacent rest atom. This is consistent with the conclusion from our experimental evidences and DFT calculation results.

V. Conclusions

The formation of (Si)$C^3H_2-C^2H$═C^1═N(Si)-like surface intermediates in acrylonitrile chemisorption on Si(111)-7 × 7 is clearly demonstrated in our HREELS, XPS, UPS, STM, and DFT studies. The surface reaction occurs mainly through a

(48) Liu, H.; Hamers, R. J. *Surf. Sci.* **1998**, *416*, 354−362.
(49) Hovis, J. S.; Hamers, R. J. *J. Phys. Chem. B* **1997**, *101*, 9581−9585.
(50) Hamers R. J.; Hovis J. S.; Lee S.; Liu, H. B.; Shan, J. *J. Phys. Chem. B* **1997**, *101*, 1489−1492
(51) Hamers, R. J.; Hovis, J. S.; Greenlief, C. M.; Padowitz, D. F. *Jpn. J. Appl. Phys.* **1999**, *38*, 3879−3887.
(52) Hovis, J. S.; Coulter, S. K.; Hamers, R. J.; D'Evelyn, M. P.; Russell, J. N.; Butter, J. E. *J. Am. Chem. Soc.* **2000**, *122*, 732−733.
(53) Liu, Q.; Hoffman, R. *J. Am. Chem. Soc.* **1995**, *117*, 4082−4092.
(54) Chadi, D. J. *Phys. Rev. Lett.* **1979**, *43*, 43−47.
(55) Hukka, T. I.; Pakkanen, T. A.; D'Evelyn, M. P. *J. Phys. Chem.* **1994**, *98*, 12420−12430.
(56) Kuang, Y. L.; Wang, Y. F.; Lee, N.; Badzian, A.; Badzian, T.; Tsong, T. T. *Appl. Phys. Lett.* **1995**, *67*, 3721−3723.
(57) Cao, X.; Hamers, R. J. *J. Am. Chem. Soc.* **2001**, *123*, 10988−10996.

[4 + 2]-like cycloaddition pathway between the adjacent adatom−rest atom pair and the two terminal atoms (C^3 and N) of the molecule. Investigation of the thermal evolution shows that the chemisorbed surface species is stable up to ∼400 K. The cumulative double bond (C═C═N) formed on the surface may be employed as a precursor to further chemical modification and functionalization of silicon surfaces or as an intermediate for dry organic syntheses.[58−61]

JA012563W

(58) Barker, M. W.; McHenry, W. E. In *The Chemistry of Kentenes, Allenes, and Related Compounds*; Patai, S.; Ed.; Wiley-Interscience: New York, 1982.
(59) McCarthy, D. G.; Hegarty, A. F. *J. Chem. Soc., Perkin Trans.* **1980**, *2*, 579−591.
(60) Patai, S. *The Chemistry of The Carbon−Nitrogen Double Bond*; John Wiley & Sons: London, New York, Toronto, 1970.
(61) Kroto, H. W.; Matti, G. Y.; Suffolk, R. J.; Watts, J. D.; Rittby, M.; Bartlett, R. J. *J. Am. Chem. Soc.* **1990**, *112*, 3779−3784.